

Studies on capacity fade of lithium-ion batteries

D. Zhang^a, B.S. Haran^a, A. Durairajan^a, R.E. White^a, Y. Podrazhansky^b, B.N. Popov^{a,*}

^a Center for Electrochemical Engineering, Department of Chemical Engineering, University of South Carolina, Columbia, SC 29208, USA

^b Advanced Charger Technology, Inc., 680 Engineering Drive, Suite 180, Norcross, GA 30092, USA

Received 14 January 2000; accepted 17 February 2000

Abstract

The capacity fade of Sony 18650S Li-ion cells has been analyzed using cyclic voltammetry, impedance spectroscopy and electron probe microscopic analysis (EPMA). The surface resistance at both the positive (LiCoO₂) and negative (carbon) electrodes were found to increase with cycling. This increase in resistance contributes to decreased capacity. Impedance data reveal that the interfacial resistance at LiCoO₂ electrode is larger than that at the carbon electrode. The impedance of the positive electrode (LiCoO₂) dominates the total cell resistance initially and also after 800 charge–discharge cycles. EPMA analysis on carbon electrodes taken from the fresh and cycled cell show the presence of oxidation products in the case of cycled cells. No change in the electrolyte resistance is seen with cycling. © 2000 Elsevier Science S.A. All rights reserved.

Keywords: Lithium-ion battery; Capacity fade; Electrochemical impedance spectroscopy; Surface film

1. Introduction

Lithium-ion rechargeable batteries with LiCoO₂ cathode and carbon anodes are rapidly replacing other battery systems due to their high energy and power densities. While the discharge properties and safety issues with these batteries have been studied in detail, not much attention has been placed on the capacity fade due to cycling. This capacity fade is caused by various mechanisms, which depend on the electrode materials and also on the charge–discharge protocol [1–3].

In general Li-ion cells have excess active material (Li⁺) in the positive electrode. This is needed to form a stable film on the electrode surfaces. It is well known that during the formation period, active Li material is lost to passivate the negative carbon electrode. This irreversible reaction seen in the initial charging cycle leads to the formation of a stable passive film on the anode. No further loss of Li is seen in subsequent cycles. However, commercial Li-ion cells lose capacity continuously. This capacity fade is accompanied by an increase in the internal impedance of the battery upon cycling. These results indicate that factors other than the irreversible reaction at the anode contribute

to the capacity decay of the Li-ion cell. Therefore, it is critical to clarify the contribution of each of the components in the cell to the whole internal impedance of the battery.

Ambiguity exists in the published literature in determining which electrode is more important for the resistance of a whole cell [4–6]. Care must be taken in interpreting electrochemical impedance spectroscopy (EIS) results since frequently several model circuits may fit the data and model circuit element may be identified with the wrong interpretation. Nyquist plots of Li-ion cells show two semi-circles with the semi-circle at low frequencies being larger in magnitude. Isaacson et al. [4] and Ganesh et al. [5], based on impedance data, claimed that the larger impedance comes from anode/electrolyte interface. However, Ozawa [6] and Megahed and Scrosati [7] assigned the larger impedance to the cathode/electrolyte interface. Since, the larger impedance contributes significantly to the loss in capacity, it is critical to identify its source.

Objectives of this study were to clear the abovementioned ambiguity and to determine the mechanism of the capacity fade of Sony lithium-ion batteries during continuous cycling. Using EIS, the change of resistance at the positive and negative electrodes was estimated at different cycle numbers. Data from the individual electrodes have been compared with that from the Sony US18650S cell. Cyclic voltammograms and charge–discharge studies were also done to complement the impedance data.

* Corresponding author. Tel.: +1-803-777-7314; fax: +1-803-777-8265.

E-mail address: popov@engr.sc.edu (B.N. Popov).

2. Experimental

All experimental studies were done on Sony US18650S cells. The batteries were charged by a constant current–constant voltage (CC–CV) charging protocol. The cell was charged at a constant current of 1 A until the potential reached 4.2 V. Subsequently, the voltage was held constant at 4.2 V to complete charging. The total charging time was 3 h. Discharge was carried out at the same current of 1.0 A within the voltage range of 4.2 to 2.5 V. Cycling studies were carried out using Arbin Battery Test (BT-2043) System. Solartron SI 1255 HF Frequency Response Analyzer and Potentiostat/Galvanostat Model 273A were used for the electrochemical characterization of Sony US18650S cells. The impedance studies were carried out on cells that were previously kept at open circuit for 1 hour in order to stabilize the cell voltage. The cell voltage changed less than 1 mV during the experiments. EIS measurements were done on the Sony cells after 50, 100, 150, 200, 250, 300, 750 and 800 cycles. Impedance studies were done on the cells at both charged and discharged states. The impedance data generally covered a frequency range of 0.002 to 5000 Hz. The frequency of the AC signal was 5 Hz.

In order to identify the contribution of the positive and negative electrodes to the total cell impedance, studies were done on the individual electrodes. Cans of cycled Sony US18650S cells were opened at the fully discharged state in a glove box filled with ultra pure argon (National Gas and Welders). Both the positive (LiCoO_2) and negative (carbon) electrodes were removed from the cell. Cylindrical discs with a diameter of 1.2 cm (an area of 1.13 cm^2) were cut from the removed electrodes. Since in the original battery, the active materials are coated on both sides of the current collectors (Cu foil for carbon or Al for LiCoO_2), the material on one side of the disc was removed to reflect similar conditions in the Sony cells. Electrochemical characterization of these individual discs was done in T-cell using a three-electrode setup. Li/Li^+ was used as the reference and lithium foil served as the counter electrode. The working electrode was the cylindrical disc cut from the Sony batteries.

Electrolyte used was 1 M LiPF_6 in a 1:1:3 mixture of propylene carbonate (PC), ethylene carbonate (EC), and dimethyl carbonate (DMC). Similar EIS studies as described above for the cell were also done on the individual electrodes in the T-cells. More details regarding the T-cells construction were described previously [8].

3. Results and discussion

3.1. Charge–discharge characteristics

Fig. 1 shows the typical C/2 rate charge–discharge profiles for different Sony US18650S cells. As shown in

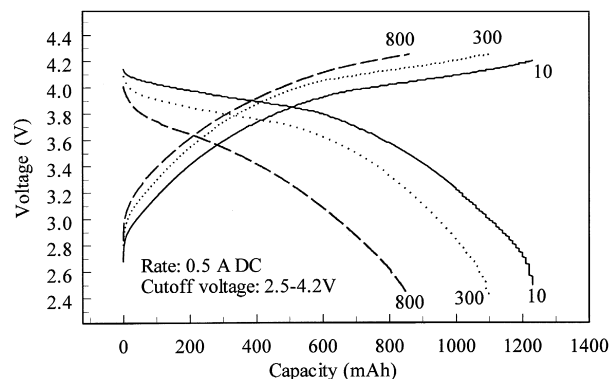


Fig. 1. Charge–discharge profiles for a Sony US18650S cell after various cycle numbers. The experiments were carried out using a constant current of 0.5 A with cutoff voltage range of 2.5–4.2 V.

Fig. 1, there are no apparent plateaus in the voltage curves. The portion of the curve at high voltages is flatter than the portion at lower voltages. It is seen in Fig. 1 that the charge–discharge capacity decreases with cycling. The initial capacity of a fresh battery during charge cycle is 1250 mAh, while during discharge is 1240 mAh. In this study, charge–discharge profiles after 10 cycles are presented instead of the first cycle, since Li-ion cells generally have different starting voltages during the first cycle.

During charge, Li^+ intercalates into the carbon electrode (reduction), and the anode potential moves from 1.2 V to approximately 0 V. Simultaneously, LiCoO_2 is oxidized (de-intercalation) and its potential changes from 3.0 to 4.2 V. During discharge, the reverse of the above occurs. While the basic shape of the charge or discharge curves remains the same over cycling, the charge or discharge capacity decreases with increasing cycle number.

Discharge capacities as a function of cycle number for Sony US18650S cells are shown in Fig. 2. After 800 cycles, the discharge capacity drops to 840 mA h, a large capacity loss occurring after extended cycling. As shown in Fig. 2, the capacity decreases continuously at a rate of 0.04% per cycle.

3.2. Cyclic voltammograms

Fig. 3 shows a comparison of cyclic voltammograms of Sony US18650S cells before and after cycling. The forward scan is associated with charging the cell and the reverse with discharging the battery. As shown in Fig. 3, peaks appear during both the charge and discharge processes. However, the characteristic peak and subsequent relaxation in current, due to diffusion limited processes, which is seen in the reverse scan (discharge), is absent during the forward sweep. This indicates that there are no limitations in inserting Li^+ into carbon and also in removing it from the cathode. The CVs in Fig. 3 were obtained with LiCoO_2 as the working electrode and carbon as both the counter and reference electrodes. As mentioned previ-

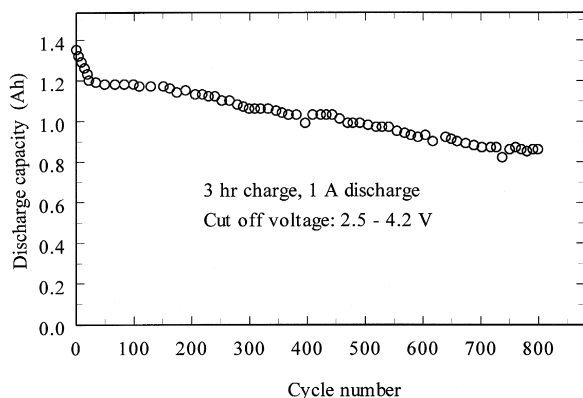


Fig. 2. Discharge capacities as a function of cycle number for Sony US18650S cells. The capacities were obtained within voltage range of 4.2–2.5 V after 3-h charging.

ously, Li-ion cells are constructed with an excess amount of Li^+ in the cathode. Since LiCoO_2 has sufficient amount of active material to completely intercalate carbon, no peaks are seen during the forward scan. The peak during the reverse scan occurs at 3.74 V. This indicates limitations of either Li^+ de-intercalation from carbon or Li^+ insertion into the cathode. While the profile of the CVs does not differ with cycling, the magnitude of the peak currents changes drastically. The peak current during charge (forward scan) decreases to 0.24 A after 800 cycles, compared to the initial value of 0.42 A. Similarly, the discharging peak current drops to 0.17 A from its initial value of 0.34 A.

Next, CV studies of individual electrodes were carried out using a T-cell. Fig. 4 presents the cyclic voltammograms obtained from the LiCoO_2 electrode. Data from electrodes in a fresh cell and also one that was cycled 800 times are shown. The forward sweep (3.0 to 4.2 V) in this case corresponds to Li^+ de-intercalation, which is equivalent to charging the Li-ion cell. Comparing the data with those shown in Fig. 3, it can be seen that the CV for the fresh cell shows peaks in current and subsequent relaxation for both the forward and reverse sweeps. Since in this case

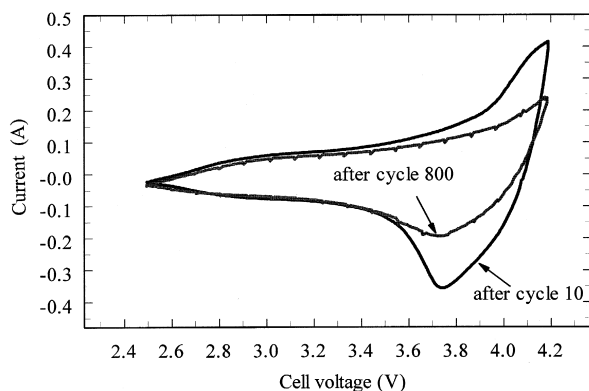


Fig. 3. Comparison of cyclic voltammograms of Sony US18650S cells. Scan rate is 0.05 mV/s with cutoff voltages of 2.5 and 4.2 V.

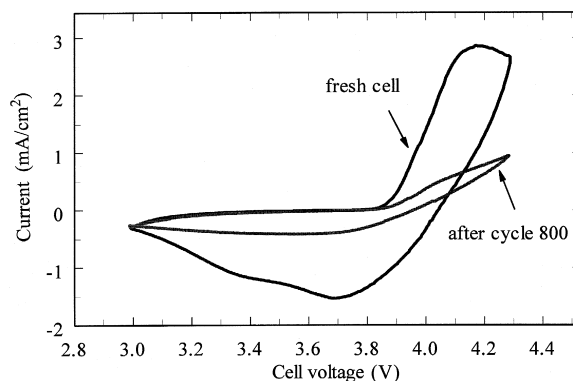


Fig. 4. Cyclic voltammograms of LiCoO_2 electrode at different cycles. Scan rate is 0.1 mV/s with cutoff voltages of 2.5 and 4.2 V.

Li is used as the counter electrode, all the active material from LiCoO_2 is removed and peaks appear during the forward scan. During the reverse sweep, the peak current appears at 3.7 V, which indicates that a similar peak seen in Fig. 3 corresponds to Li^+ intercalation into LiCoO_2 . This peak current is not prominent after 800 cycles. Further, the magnitude of the currents decreases during cycling, which is in agreement with the data shown in Fig. 3. The drastic reduction in current indicates changes in the surface of the LiCoO_2 electrode with cycling. This change in surface layer could have increased the positive electrode resistance, thereby decreasing the charge and discharge currents seen in Figs. 3 and 4. The peaks seen during initial cycles arise from limitations in transport of Li^+ as compared to the fast reaction rates. The increase in film resistance contributes to a lower reaction rate at the electrode/electrolyte interface. Hence, the current peaks vanish with cycling.

Fig. 5 presents cyclic voltammograms obtained for the carbon electrode using a T-cell. The potential was initially swept from 1.2 to 0 V and then back during the reverse sweep. The forward scan (sweep to 0 V) corresponds to Li^+ intercalation into carbon and is equivalent to charging

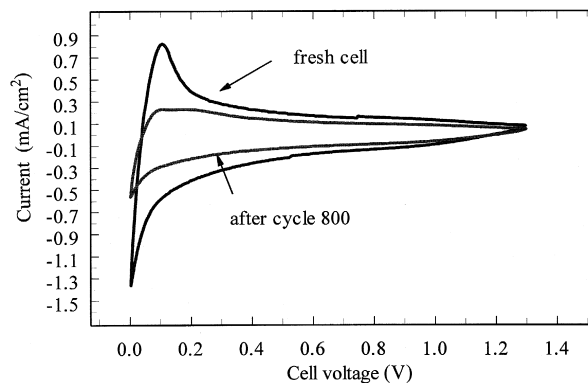


Fig. 5. Cyclic voltammograms of the carbon electrode from a fresh Sony cell and from one after 800 charge-discharge cycles. Scan rate is 0.1 mV/s with cutoff voltages of 0.0 and 1.3 V.

the Li-ion cell. The currents increase as the potential is shifted closer to 0 V. Increasing the potential beyond this value would result in Li deposition. The kinetics for this reaction are very fast and the overcharge phenomena and subsequent loss of capacity due to this has been studied extensively. During the reverse sweep a peak appears at 0.08 V. This indicates that the kinetics for Li^+ de-intercalation are very fast and mass transfer limitations set in very early. However, this peak vanishes after 800 cycles and the magnitude of the currents is also lower. Similar results were also seen in Fig. 4 for the positive electrode. A similar mechanism, as for LiCoO_2 (an increase in surface film resistance), can be postulated to account for the reduction in charge–discharge currents and the absence of discharge peaks with cycling. Finally, a comparison of cyclic voltammograms in Fig. 4 and Fig. 5 indicates that the LiCoO_2 electrode deteriorates more severely than the carbon electrode over cycling.

Fig. 6a and 6b present the cyclic voltammograms of the positive electrode initially and after 800 cycles, respectively. Data for the individual LiCoO_2 electrode have been collected at different scan rates. From Fig. 6a, it is clear that the peaks seen during Li^+ intercalation (sweep from 4.2 to 3.0 V) shift depending on the scan rate. The peak appears at more positive potentials as the sweep rate is

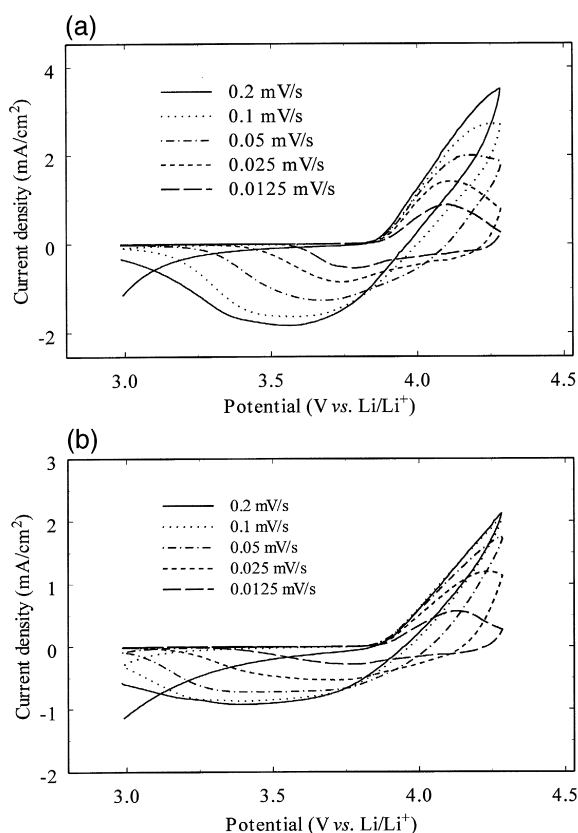


Fig. 6. Cyclic voltammograms of LiCoO_2 electrode at different scan rates — (a) electrode from a fresh cell and (b) electrode after 800 charge–discharge cycles.

lowered. Similarly, the potential at which Li^+ intercalation begins also shifts to more positive potentials (approximately 250 mV shift from 0.0125 to 0.2 mV/s) at lower scan rates. These results can be explained by taking into account the simultaneous effects of mass transfer and reaction. At high sweep rates, sufficient time is not allowed for Li^+ to entirely de-intercalate from the electrode. Due to diffusion limitations, not all Li^+ have been removed from the LiCoO_2 electrode. This is reflected by the positive currents, corresponding to Li^+ de-insertion seen during the initial phase of the reverse sweep at high scan rates. At low sweep rates, most of the Li^+ has been removed from LiCoO_2 and the electrode equilibrium potential is more positive. Hence, on reversing the sweep, the current polarity immediately changes (positive to negative) corresponding to Li^+ intercalation. The same effect causes the shift of the peak currents during the reverse sweep. At low scan rates, the time for Li^+ insertion is large and hence the peak appears much earlier as compared to high sweep rates.

Similar behavior is seen in Fig. 6b after 800 charge–discharge cycles. However, no peaks are seen during the reverse sweep at high scan rates. This is in agreement with the results presented in Figs. 3 and 4. Integrating the charge and discharge capacities in Fig. 6a and 6b reveals a loss in capacity with cycling. The SEI formed on the LiCoO_2 is due to the side reactions occurring at the electrode surface during cycling. When the electrodes are in charged state, a large portion of Co^{4+} cations with strong oxidizing power will be present in the cathode, which will react with the electrolyte at the interface. After extended cycling, the LiCoO_2 electrode surface is heavily passivated resulting in a large resistance at the interface. This increased resistance contributes to a lower reaction rate for both Li^+ insertion and de-intercalation. The absence of peaks (except at very low scan rates) can be attributed to this reduced reaction rate.

The results presented here are preliminary in nature and the hypothesis of change in film resistance needs to be substantiated further. This has been accomplished by data obtained from impedance studies.

3.3. Impedance studies

The Nyquist plots obtained for a fresh Sony cell are shown in Fig. 7a. The overall cell impedance is much larger during discharge as compared to the charged state. The impedance data reveal two distinct semi-circles with the semi-circle at low frequencies increasing in magnitude during discharge. The electrolyte resistance (real part of the impedance) remains constant (0.205 Ω) during charge and discharge. In order to identify the contribution of the individual electrodes to the total cell impedance, studies were done separately on T-cells. These data are shown in Fig. 7b and 7c at the discharged and charged state, respectively.

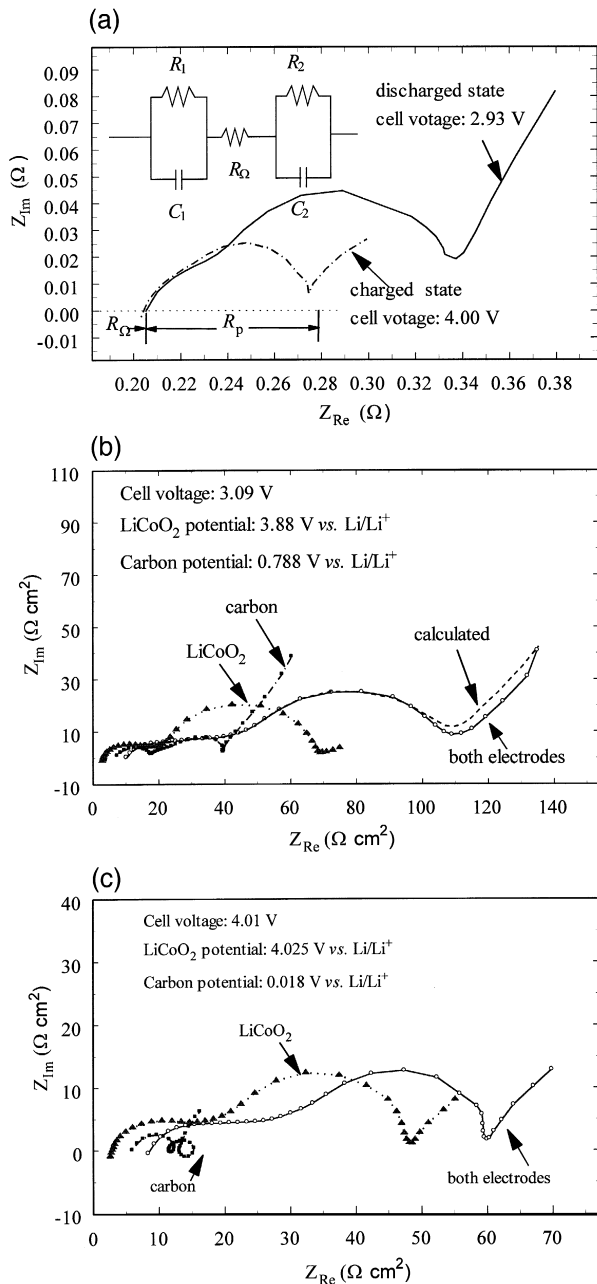


Fig. 7. Nyquist plots for fresh Sony cells (a) complete cell (b) electrodes at discharged state and (c) electrodes at charged state. The resistances have been normalized with respect to the electrode area.

From Fig. 7b, the normalized total resistances are $39 \Omega \text{ cm}^2$ for carbon electrode, $68 \Omega \text{ cm}^2$ for LiCoO_2 electrode and the total resistance is $107 \Omega \text{ cm}^2$ for both electrodes. The resistances have been normalized with respect to the electrode area using the equivalent circuit presented in Fig. 7a. The total resistance of carbon electrode is the sum of the following resistances: (i) electrolyte solution resistance (R_Ω), (ii) surface layer resistance or the carbon particle to particle contact resistance (R_1), and (iii) the charge transfer resistance (R_3). The resistances for the LiCoO_2 are similar to that of the carbon electrode.

In Fig. 7b, the normalized resistance of a fresh Sony 18650S cell at the discharged state is also shown for comparison. The curve labeled *calculated* was obtained by summation of the impedance response for carbon and that for LiCoO_2 electrode according to Eq. (1).

$$Z_{\text{Re}} = Z_{\text{Re,LiCoO}_2} + Z_{\text{Re,carbon}};$$

$$Z_{\text{Im}} = Z_{\text{Im,LiCoO}_2} + Z_{\text{Im,carbon}} \quad (1)$$

The calculated curve agrees well with the measured one, especially at high frequencies. From the data shown in Fig. 7b, it is clear that the LiCoO_2 electrode contributes more to the total resistance of the cell. This is proven by the close matching of the *calculated* curve with the cell data.

Fig. 7c shows a comparison of the Nyquist plots obtained using a T-cell and the Sony 18650S cell at the charged state. The normalized total resistances are $15 \Omega \text{ cm}^2$ for carbon electrode, $48 \Omega \text{ cm}^2$ for LiCoO_2 electrode, and $62 \Omega \text{ cm}^2$ for both electrodes. Again, it is clear that the LiCoO_2 electrode contributes more to the total resistance of the cell. A comparison of Fig. 7b and c indicates that interfacial impedance at the discharged state is larger when compared with the charged state for both carbon and LiCoO_2 electrodes. The results shown here clearly prove that the impedance of Li-ion cells with LiCoO_2/C electrodes is dominated by the positive electrode. Further, it is also clear the total cell impedance increases with decrease in SOC. Our next objective was to study the change in these impedance profiles with cycling.

Typical Nyquist plots obtained for Sony cells after every 50 or more charge–discharge cycles are summarized in Fig. 8. The impedance responses were measured at an open circuit voltage of 3.6 V. The observed semicircles were highly reproducible; of more than 50 impedance–response spectra collected from Sony cells at different states of charge and at different cycle numbers, each one showed similar feature. However, the relative size of the semicircles was found to depend on the previous history of the cell; both semicircles were generally found to increase in

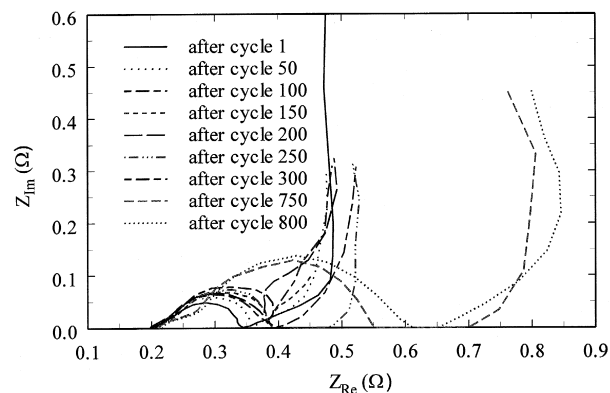


Fig. 8. Typical Nyquist plots obtained for Sony cells after every 50 or more charge–discharge cycles. The impedance responses were measured at open circuit voltage of 3.6 V.

size with increasing the cycle number. As shown in Fig. 8, while the Nyquist plots were basically similar in shape, their sizes change. The increase in cell resistance indicates change in resistance of the individual cell components.

Some of the processes that are known to lead to capacity fade in lithium-ion cells are lithium deposition (over charge conditions), electrolyte decomposition, active material dissolution, phase changes in the insertion electrode materials, and passive film formation over the electrode and current collector surfaces [3]. In a Sony lithium-ion battery, the side reactions are associated with each of the components in the battery. Since both of the current collectors (Al and Cu foils) in commercial lithium-ion cells are pretreated to improve their adhesion properties and to reduce corrosion rates [3], the resistance due to the passive film formation on the current collector surfaces is invariant and negligible. This was verified by our EIS measurements on Al and Cu current collector after extended cycling of the Sony batteries [9]. Since the negative electrode material of the test battery is metallic (carbon behaves like metal electrically), its contribution to the overall ohmic resistance should be negligible and its electrical conductivity is not expected to change with cycling. On the other hand, the positive electrode of the test battery comprising Li_xCoO_2 is a semiconductor, and its conductivity should

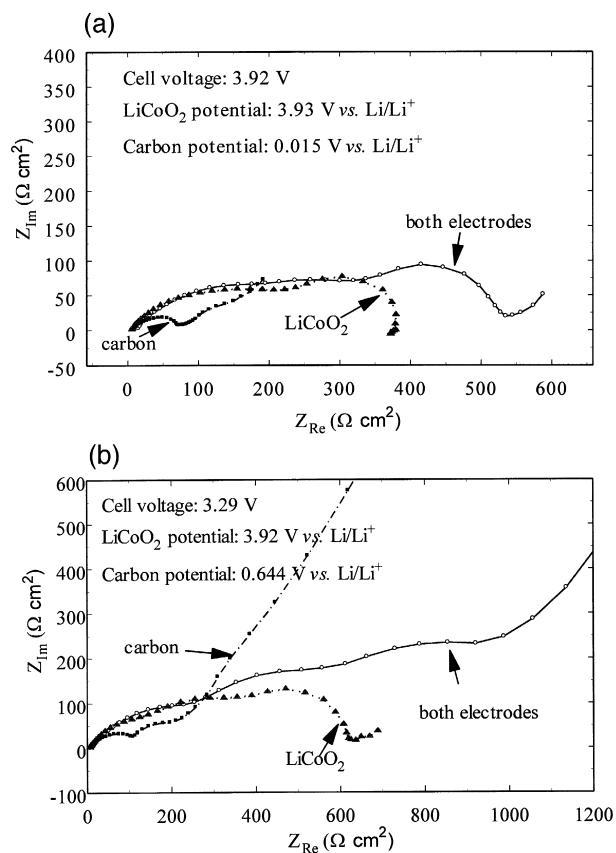


Fig. 9. Nyquist plots obtained using a T-cell at (a) charged state and (b) discharged state. The electrodes and separator are from the Sony US18650S cell that has been cycled 800 cycles.

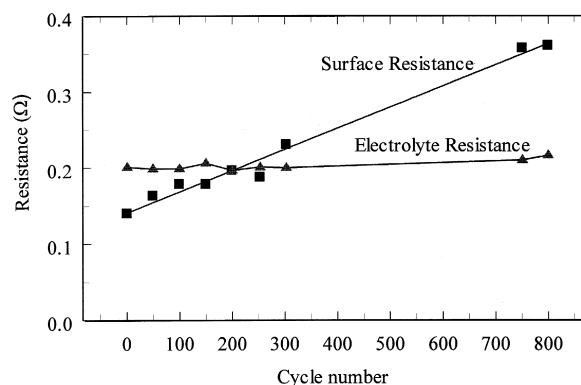


Fig. 10. The change in electrolyte, and total surface layer resistance of a Sony US18650S cell as a function of cycle number.

also be invariant with cycling when it is measured at a certain voltage, i.e. when the lithium-ion content in the Li_xCoO_2 solid matrix is kept at a certain level [5]. Ionic conductivity does not contribute significantly to the measured conductivity [12]. Thus, the factors affecting the impedance are related directly to the electrode materials and their interactions with electrolyte.

Fig. 9a and 9b show Nyquist plots for the Sony cell cycled 800 times at the charged and discharged states, respectively. Impedance data have been obtained from individual electrodes in a T-cell. Data obtained with the complete Sony 18650S cell is also shown for comparison. The electrodes and separator are from the Sony US18650S cell that has been cycled 800 times. The normalized total resistances in the charged state are $74 \Omega \text{ cm}^2$ for carbon electrode, $384 \Omega \text{ cm}^2$ for LiCoO_2 electrode, and $530 \Omega \text{ cm}^2$ for both electrodes. The normalized total resistances in the discharged state are $240 \Omega \text{ cm}^2$ for carbon electrode, $610 \Omega \text{ cm}^2$ for LiCoO_2 electrode, and $900 \Omega \text{ cm}^2$ for both electrodes. It is interesting to compare the EIS responses of Fig. 7a–c with those of Figs. 8 and 9. As expected, there are some similarities between them. The resistance during discharge remains higher than that at the charged state, even after 800 cycles. The normalized interfacial resistance is $62 \Omega \text{ cm}^2$ for the fresh Sony cell at 4.00 V (Fig. 7c), compared to $530 \Omega \text{ cm}^2$ for both electrodes after 800 cycles (Fig. 9a). The shape of the curves in both cases is similar. However, the resistance increases at both the anode and cathode. Since the salt in the electrolyte does not participate in the overall cell reaction, its composition and hence its conductivity does not change during cycling. This is reflected by the small displacement of the semi-circles after 800 cycles. It can be clearly seen from Fig. 8 that LiCoO_2 deteriorates rapidly and causes significantly to the overall increase of the cell impedance. The resistance due to LiCoO_2 increased about 10 times in value with cycling and that due to carbon electrode increased about eight times. While, the change in carbon resistance is also important, increases in the positive electrode resistance overshadow this. These studies

Table 1
Change in resistance of LiCoO₂ and carbon with cycling

Electrode	Electrolyte resistance (Ω cm ²)	Surface layer resistance (Ω cm ²)	Polarization resistance (Ω cm ²)
LiCoO ₂ (fresh)	3	17.7	51.7
Carbon (fresh)	7.2	12.3	24.6
LiCoO ₂ (after 800 cycles)	4.5	305.2	340.6
Carbon (after 800 cycles)	6.2	145.7	184.9

conclusively prove that LiCoO₂ contributes most to the resistance of the Sony 18650S cell and also contributes most to the capacity decay.

Fig. 10 shows changes in the total surface resistance of LiCoO₂ and carbon and the electrolyte resistance with cycling (Table 1). While it is clear that the resistance of both the positive and negative electrodes increases with cycling, it is not clear what causes this increase. The cycling reversibility of a Li-ion battery depends on the stability of the electrodes immersed in an electrolyte that in turn depends on the mechanism of the side reactions occurring at the electrode/electrolyte interfaces. In addition to LiPF₆ as salt, PC, DMC and methyl ethyl carbonate (MEC) are the components of the electrolyte in the Sony 18650 Li-ion cell, which uses coke-based anodes [1]. The interactions among the anode, cathode and electrolyte result in formation of SEI. Accordingly, analysis of the side

reactions may help to elucidate the mechanism of capacity fade [13]. From Fig. 10, it is clear that the conductivity of the electrolyte is not affected due to these side reactions.

It is well known that the irreversible capacity loss in Li-ion batteries is significant during first charge–discharge cycle due to the irreversible capacity loss in the carbon electrode [10]. The SEI on carbonaceous electrode consists of many different materials including LiF, LiCO₃, LiCO-R, Li₂O, lithium alkoxides, nonconductive polymers, and more [11]. Since an optimized SEI can be formed on the surface of carbon electrode during initial cycles [11], the capacity loss due to impedance on carbon electrode is very small during later cycles. In other words, the carbon electrode causes capacity fade of the lithium-ion cells mainly during formation cycles, which were done by the manufacturers [3,10].

The implication of the SEI on the carbon electrode is twofold in the capacity fade [14,15]. First, it will cause a voltage drop over the SEI. Second, it will modify the structure of the double layer at the electrode/electrolyte interface and generally increase the charge transfer resistance at this interface. Electron probe microscopic analysis (EPMA) was used to determine the concentrations of some of the constituent elements such as oxygen and fluorine in the carbon samples extracted from the negative electrode of fresh and cycled lithium-ion cells. EPMA measures the characteristic X-ray spectrum of the specimen and compares it with the known standard intensities of constituent by way of maps. The map uses a scale that corresponds to

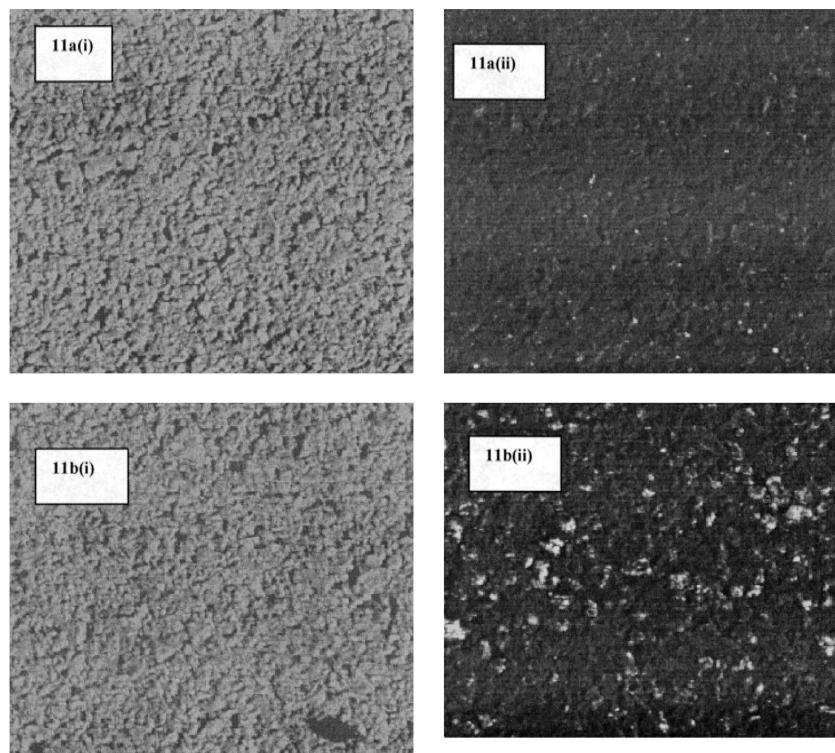


Fig. 11. EPMA analysis on carbon electrode extracted from (a) fresh electrode and (b) after 800 cycles.

a black body radiation with concentration equated to temperature. Fig. 11 shows EPMA results obtained on carbon electrodes taken from fresh and cycled cells. It was found that the oxygen content in the carbon electrode increases from 4.9% in case of fresh cell (Fig. 9a [ii]) to approximately 14.2% in case of DC-charged Sony cell (Fig. 9b [ii]). Fluorine content was also analyzed (not shown) and the percentage content changed only slightly from 4% in the case of fresh cell to about 4.2% in case of cycled cells. The concentrations shown in Fig. 11 were normalized to the sum of actual concentrations of carbon, fluorine and oxygen. The EPMA results are in agreement with impedance data. The observed increase in the oxygen content with cycling is due to the surface electrode oxidation, which results in an increase of the interfacial resistance. The increase in resistance at the carbon electrode will result in an increase in the electrode potential from 0 V to more positive potentials in the charged state. Since the cell is cycled between 2.5 and 4.2 V, this would cause the actual potential at the LiCoO_2 electrode to be much higher than 4.2 V. Increase in potential at LiCoO_2 -electrolyte interface would cause oxidation of the active material, thereby increasing the surface resistance. It was reported that the resistance of the SEI increases with time for $\text{LiCoO}_2/\text{LiBF}_4$ system in PC and a direct evidence was seen by electron microscope image [14,15]. This could contribute to the loss in capacity with cycling. Apart from this, damage and disorder in LiCoO_2 particles induced by cycling will also cause capacity fade [16]. Cycling induces severe strain, high defect densities and occasional fracture of particles and severely strained particles exhibit cation disorder [16]. These will lead to change in thermodynamic properties and contact resistance of the LiCoO_2 particles. The accumulation of strain in the particles may cause partial shedding of the electrode sheet from its current collector. A portion of the lithium-ions in the cathode can become inactive due to cation disordering. However, the capacity fade in the LiCoO_2 electrode is mainly caused by the change in resistance on the surface of the particles.

4. Conclusions

The capacity fade of commercial Li-ion cells (Sony 18650S) has been studied in detail. After 800 cycles, the discharge capacity of the Sony 18650S cell drops to 840 from 1200 mA h, a large capacity loss occurring after extended cycling. Cyclic voltammetry and impedance spectroscopy have been used to study the decay in performance of the batteries with cycling. CVs of LiCoO_2 and carbon electrodes indicate an increase in the interfacial resistance with cycling. It is seen that LiCoO_2 deteriorates more severely than the carbon electrode during cycling. To confirm these results, impedance spectroscopy was used to

determine the interfacial impedance parameters as well as the internal ohmic resistance of Sony lithium-ion batteries at different charge–discharge cycles. After cycling, the can of the battery was opened and the individual electrode parameters were determined. The total cell resistance varies significantly with SOC, with resistance being higher at the discharged state. It is also seen that the impedance of the positive electrode dominates the total cell resistance. No significant change in the electrolyte resistance is seen with cycling. However, both the positive and negative electrode resistances increase with cycling, thereby increasing the total cell impedance. Finally, the positive electrode (LiCoO_2) contributes more to the capacity fade of the lithium-ion cells, when compared to the negative electrode. This increase in impedance of LiCoO_2 electrode with cycling is attributed to an increase in surface resistance due to oxidation.

Acknowledgements

Financial support provided by DOE Division of Chemical Sciences, Office of Basic Energy Sciences G.M. DE-FG02-96ER 146598 is acknowledged gratefully.

References

- [1] B. Johnson, R.E. White, *J. Power Sources* 70 (1998) 48.
- [2] D. Linden (Ed.), *Handbook of Batteries*, 2nd edn., McGraw-Hill, New York, 1995, pp. 36.44–36.48.
- [3] P. Arora, R.E. White, M. Doyle, *J. Electrochem. Soc.* 145 (1998) 3647.
- [4] M.J. Isaacson, M.E. Daman, R.P. Hollandsworth, *Proc. 32nd International Society Energy Conversion Engineering Conference 2* (1997) 31.
- [5] V. Ganesh Kumar, N. Munichantaiah, A.K. Shukla, *J. Appl. Electrochem.* 27 (1997) 43.
- [6] K. Ozawa, *S. S. Ionics* 69 (1994) 212.
- [7] S. Megahed, B. Scrosati, *J. Power Sources* 51 (1994) 79.
- [8] D. Zhang, B.N. Popov, R.E. White, *J. Power Sources* 76 (1998) 81.
- [9] D. Zhang, B.N. Popov, R.E. White, *The Electrochemical Society Meeting Extended Abstracts*, Boston, MA, Nov. 1–6, 1998. vol. 98-21998, Abstract No. 11.
- [10] Y. Matsumura, S. Wang, J. Mondori, *J. Electrochem. Soc.* 142 (1995) 2914.
- [11] E. Peled, D. Golodnitsky, C. Menachem, D. Bar-Tow, *J. Electrochem. Soc.* 145 (1998) 3482.
- [12] G. Wei, T.E. Haas, R.B. Goldner, *S. S. Ionics* 58 (1992) 115.
- [13] D. Aurbach, Y. Ein-Eli, O. Chusid, Y. Carmeli, M. Babai, H. Yamin, *J. Electrochem. Soc.* 141 (1994) 603.
- [14] M.G.S.R. Thomas, P.G. Bruce, J.B. Goodenough, *J. Electrochem. Soc.* 132 (1985) 1521.
- [15] D. Aurbach, M.D. Levi, E. Levi, H. Teller, B. Markovskiy, G. Salitra, U. Heider, L. Heider, *J. Electrochem. Soc.* 145 (1998) 3024.
- [16] H. Wang, Y.-I. Jang, B. Huang, D.R. Sadoway, Y.-M. Chiang, *J. Electrochem. Soc.* 146 (1999) 473.